

AMORPHOUS SILICON DIOXIDE LAYER FOR HIGH EFFICIENCY CRYSTALLINE SOLAR CELLS

HUSSEIN K. RASHEED & ASSMA H. MUSLIM

Baghdad University, College of Science Department of Physics, Baghdad, Iraq

ABSTRACT

High efficiency crystalline solar cells must improve performance while replacing higher cost mono crystalline silicon with lower cost multicrystalline silicon. This is being achieved through new cell device structures that improve light trapping and energy conversion capability. In crystalline silicon hetero junction solar cells, optical losses can be mitigated by using wider band gap amorphous silicon oxide (p-a-SiO₂) as window layer.

*RF sputtering was used to deposit n-a-SiO₂ with power (150w) and pressure (7.2*10⁻³). The Wider band gap of the Window layer increases the transmission of short Wavelength light into the emitter and base layers of the photovoltaic cell. This in turn increases the current generation in the photovoltaic cell. We improved an efficiency of 4.64% (active area efficiency) with an open-circuit voltage (V_{oc}) of 551.9mV.*

KEYWORDS: SiO₂, Window Layer & Solar Cell

Received: Oct 09, 2016; **Accepted:** Dec 07, 2016; **Published:** Dec 09, 2016; **Paper Id.:** IJNADEC20161

INTRODUCTION

An important prerequisite for reaching high efficiencies in crystalline silicon solar cells is good surface passivation of the wafer. This enables high voltages at open circuit (V_{oc}) but also at the maximum power point, leading to high fill factors (FF) [1]. Passivation schemes commonly used in photovoltaic applications are silicon dioxide (SiO₂), silicon nitride (SiN_x), intrinsic amorphous silicon (a-Si (i): H) and amorphous silicon carbide. SiO₂ yields a low interface state density, but is grown at high temperatures, and suffers from long term UV instability. The SiN_x passivation quality depends strongly on the used Si doping type and level [2].

The properties of doped n-a-SiO₂ films prepared by radio-frequency sputtering deposition (RF-Sputtering) and these films were applied to the doped layer of HJ-c-Si solar cells with as window showed a conversion efficiency of 4.64% [3].

EXPERIMENTAL

We first study the optical and electrical properties of the p-a-SiO₂ layers deposited on glass prior to their introduction in c-Si solar cells. The p-c-SiO₂ layers were deposited by RF Sputtering with power (150w), the deposition temperature was 64°C and the working pressure in the deposition chamber was 7.2*10⁻³ mbar. Films with a thickness of 60nm were deposited on glass substrates. Fourier Transform Infrared Spectroscopy (FTIRS) was used to determine the chemical bonding states of the films. To evaluate the contamination as well as the Si/SiO₂ interface as in the volume of the films, Atomic Force Microscopy (AFM).

RESULTS AND DISCUSSIONS

FTIRS Analysis

Figure 1 shows typical spectra of the deposited silicon oxide. We observed the regular stretching, bending and rocking absorbance bands of silicon oxide films.

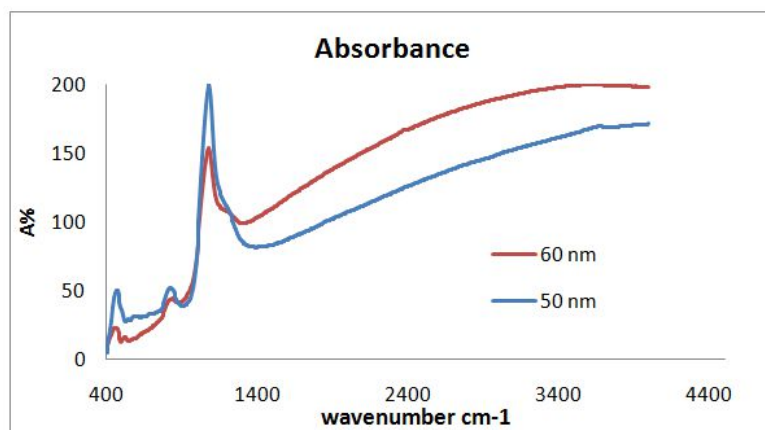


Figure 1: FTIRS Spectra of Samples Deposited with Different Thickness of SiO₂ thin Films. The Three Observed Peaks Correspond to Silicon-Oxygen Bonds.

- **AFM analysis**

Figures 2 to 5 show two and three dimensional AFM images of the surface topography of a-SiO₂ films (of different thicknesses) deposited on Si at Ta=300°C. In these images, S_a (Surface Roughness Average) is very small which shows very good smoothness of the surface. This means that the prepared films are well deposited. The values of Surface topography parameters such as Surface Roughness Average, Root Mean Square roughness, and Ten Point Height for a-SiO₂ films at different thicknesses.

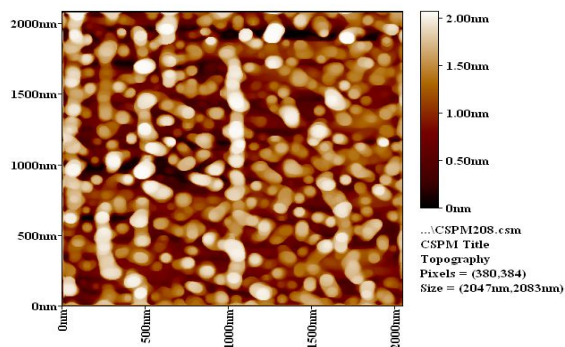


Figure 2: 2-D AFM Image of Surface Topography of CdTe Film with 60nm Thickness Deposited on SI at Ts=RT and Annealed at Ta=300°C

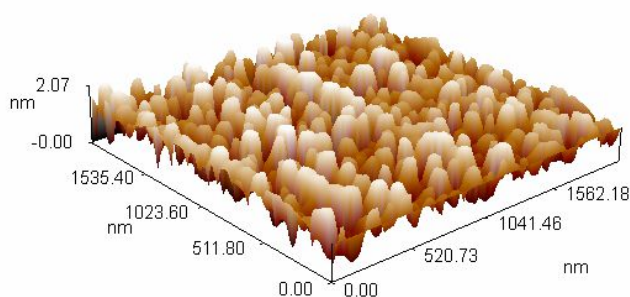


Figure 3: 3-D AFM Image of Surface Topography of a-SiO₂ Film with 60nm Thickness Deposited on Si at Ts=RT and Annealed at Ta=300°C

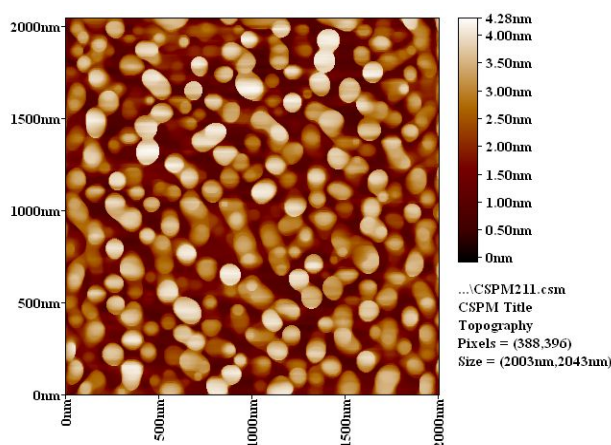


Figure 4: 2-D AFM Image of Surface Topography of a-SiO₂ Film with 50nm Thickness Deposited on Si at Ts=RT and Annealed at Ta=300°C

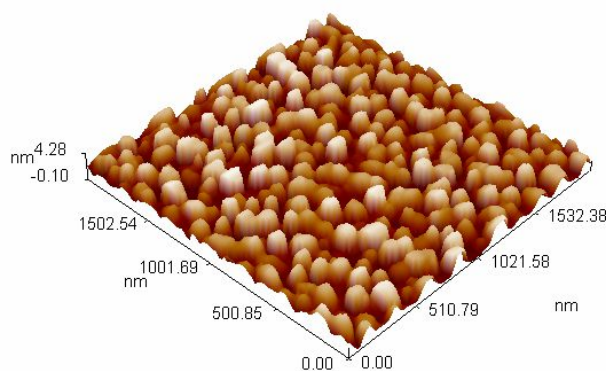


Figure 5: 3-D AFM Image of Surface Topography of a-SiO₂ FILM with 50nm Thickness Deposited on Si at Ts=RT and Annealed at Ta=300°C

I-V Characteristics

The I-V characteristics were measured to evaluate electrical properties of a-SiO₂/c-Si films. As shown in Figure 4, we can see the improvement of efficiency up to 4.64% (active area efficiency) with an open-circuit voltage (V_{oc}) of 551.9mV.

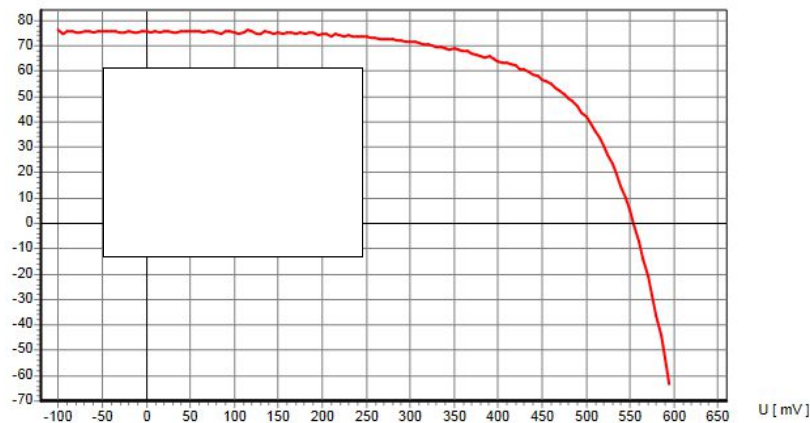


Figure 6: I-V Curve for c-Si Solar Cell

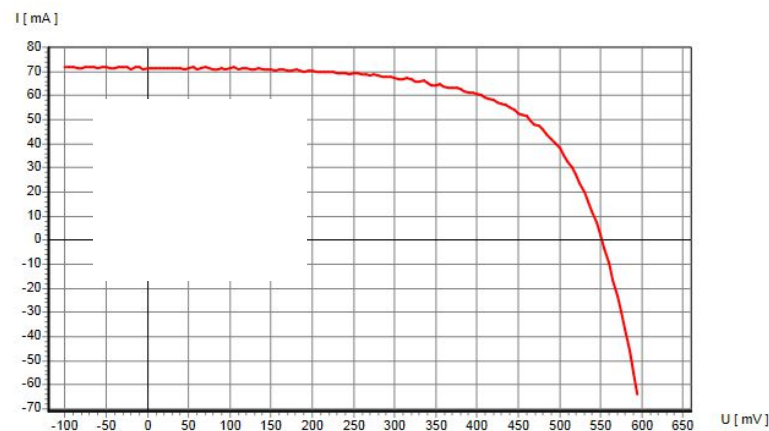


Figure 7: I-V curve for a- SiO₂/c-Si solar cell in which the thickness of SiO₂ film is 50nm

CONCLUSIONS

The present invention consists of a Wide band gap semiconductor used in the Window layer of a photovoltaic cell. The Wider band gap of the Window layer increases the transmission of short wavelength light into the emitter and base layers of the photovoltaic cell. This in turn increases the current generation in the cell.

We introduced and characterized the heterojunction crystalline silicon solar cells using p-a-SiO₂ as the window layers. The best solar cell shows a conversion efficiency of 4.64% ($V_{oc} = 551.9\text{mV}$, $FF = 0.619$). These results indicate that a wide gap and high-conductivity p-a-SiO₂ layer is a promising material as the window layer of HJ-c-Si solar cells.

REFERENCES

1. K. Ding et al., "Optimized amorphous silicon oxide buffer layers for silicon heterojunction solar cells with microcrystalline silicon oxide contact layers Optimized amorphous silicon oxide buffer layers for silicon heterojunction solar cells with microcrystalline silicon oxide contact layers," vol. 134501, no. May 2015, pp. 2011–2016, 2014.
2. F. Einsele, W. Beyer, U. Rau, F. Einsele, W. Beyer, and U. Rau, "Analysis of sub-stoichiometric hydrogenated silicon oxide films for surface passivation of crystalline silicon solar cells Analysis of sub-stoichiometric hydrogenated silicon oxide films for surface passivation of crystalline silicon solar cells," vol. 054905, no. 2012, 2014.

3. S. Gatz et al., "Thermal stability of amorphous silicon / silicon nitride stacks for passivating crystalline silicon solar cells Thermal stability of amorphous silicon / silicon nitride stacks for passivating crystalline silicon solar cells," vol. 173502, no. 2008, pp. 13–16, 2012.
4. J. Geissbühler et al., "22. 5 % efficient silicon heterojunction solar cell with molybdenum oxide hole collector 22. 5 % efficient silicon heterojunction solar cell with molybdenum oxide hole collector re," vol. 081601, 2015.
5. O. M. Ghahfarokhi, K. Von Maydell, and C. Agert, "Enhanced passivation at amorphous / crystalline silicon interface and suppressed Schottky barrier by deposition of microcrystalline silicon emitter layer in silicon heterojunction solar cells Enhanced passivation at amorphous / crystalline silicon interface and suppressed Schottky barrier by deposition of microcrystalline silicon emitter layer in silicon heterojunction solar cells," vol. 113901, 2014.
6. K. Lee, E. Ok, J. Park, W. M. Kim, Y. Baik, and D. Kim, "The impact of oxygen incorporation during intrinsic ZnO sputtering on the performance of Cu (In, Ga) Se₂ thin film solar cells The impact of oxygen incorporation during intrinsic ZnO sputtering on the performance of Cu (In, Ga) Se₂ thin film solar cells," vol. 083906, 2014.
7. J. V Li et al., "Influence of sputtering a ZnMgO window layer on the interface and bulk properties of Cu (In, Ga) Se₂ solar cells Influence of sputtering a ZnMgO window layer on the interface and bulk properties of Cu , In, Ga Se₂ solar cells," vol. 2384, no. 2009, pp. 1–7, 2014.

